

# DESIGN OF A PAVEMENT SOLUTION FOR ELECTRIC VEHICLE CHARGING BY INDUCTION

Pierre Hornych , Thomas Gabet & Brahim Mazhoud  
Université Gustave Eiffel, MAST, France

[pierre.hornych@univ-eiffel.fr](mailto:pierre.hornych@univ-eiffel.fr)

Eric Coquelle,

COLAS, CST, France

[eric.coquelle@colas.com](mailto:eric.coquelle@colas.com)

Zariff Meira & Karim Kadem

VEDECOM, France

[zariff.meira@vedecom.fr](mailto:zariff.meira@vedecom.fr)

## ABSTRACT

In recent years, with the rapid development of electric vehicles (EVs), the design and evaluation of different solutions for recharging these vehicles have been the subject of numerous studies. In particular, dynamic inductive charging appears as a promising charging solution, offering several advantages: no physical connection with the vehicle, no manipulation by the user during charging, and reduced risk of damage or vandalism of the system, which is integrated into the road. This paper presents the work carried out in the framework of the European project INCIT-EV (2020 -2024), aiming at developing a dynamic charging system by induction for electric vehicles (cars and light utility vehicles), intended for urban applications, with a charging power of 30 kW.

An important issue in the development of inductive charging systems is the integration into the pavement structure, to ensure the electrical efficiency, durability and traffic resistance of the inductive coils, integrated into the pavement. This article presents the studies carried out in the INCIT-EV project to design an Electric Road demonstrator, integrating an inductive charging system, to be built in Paris. Within the framework of the project, specific tests have been developed to study the mechanical and thermal behavior of this electric road. In particular, laboratory rutting tests have been carried out to study, on a reduced scale, the mechanical behavior of a recharging coil integrated into the pavement. Charging tests were also carried out to study the charging efficiency and the temperature variations produced by the heat dissipation in the charging system. These laboratory studies were complemented by finite element calculations to simulate the thermal and mechanical response of the system in the pavement structure. The studies have allowed to select appropriate materials for the integration of the inductive coils, and to propose a suitable road design for the demonstrator, which will be built in Paris in 2023.

## 1. INTRODUCTION

The INCIT-EV project [1] is a European project of the Horizon 2020 program, which aims to develop and test different charging solutions for electric vehicles, and to evaluate their perception by users. This project brings together 33 partners (industrial companies, research laboratories, project owners) and aims to develop 7 charging technology demonstrators, including several charging station technologies, and also static and dynamic on-road charging systems. As indicated on the project website [1], its objectives are to develop innovative charging systems, software platforms to control their operation, and also to evaluate their performance, through demonstrations in real conditions.

The work presented in this article is carried out within the framework of task 4 of the project, and aims at developing a solution of dynamic charging of vehicles by the road, by induction, intended for urban applications. This type of solution is commonly called Electric Road System (ERS). This solution is being developed in partnership by VEDECOM, COLAS and Université Gustave Eiffel, and will lead to the construction of a demonstrator, which will be installed in a street in Paris, and tested in real conditions of use.

Inductive charging solutions are based on the transmission of electrical energy without contact, thanks to the magnetic coupling between a primary coil installed in the roadway and a secondary coil located under the vehicle (Figure 1). Research on vehicle recharging solutions by induction (static or dynamic), has been active since the 1990s [2], [3], and today, some systems are used operationally [4].

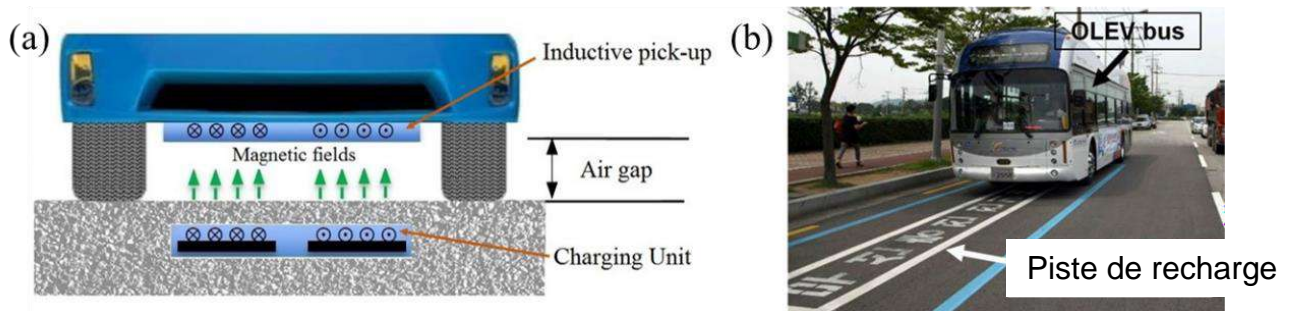


Figure 1. (a) Principle of inductive charging system (from [5])  
 (b) Charging solution for buses developed by OLEV (South Korea) [4].

An important issue in the development of inductive charging systems is also the integration into the pavement structure, to ensure at the same time the electrical efficiency, durability and traffic resistance of the Electric Road. This article summarizes these pavement integration aspects. A more complete presentation of this work can be found in the corresponding INCIT-EV project report [6].

## 2. CHARACTERISTICS OF THE CHARGING SYSTEM

In the INCIT-EV project, the inductive charging system was developed by VEDECOM. This system is designed for urban applications, and is intended for charging cars and small utility vehicles. The power supplied is 30 kW per coil. The primary part of the system (integrated in the road) includes :

- the primary coils (made of copper wires), installed in the roadway, in the middle of the lane, and at a shallow depth (about 6 cm), to minimize the distance to the secondary coils, in order to maximize charging efficiency.
- the associated power supply, which includes a transformer, which provides the DC current needed to power the system, and inverters (one per coil), which generate the high frequency AC current needed for optimal energy transfer to the vehicle.

This system is intended to be installed in an existing asphalt pavement. Figure 2 shows the planned layout: the coils are placed in the middle of the roadway, in a trench, and covered by a new surface layer. The inverters are placed in a culvert located at the edge of the road, closed by removable covers. The transformer is located on the sidewalk in the middle of the charging area.

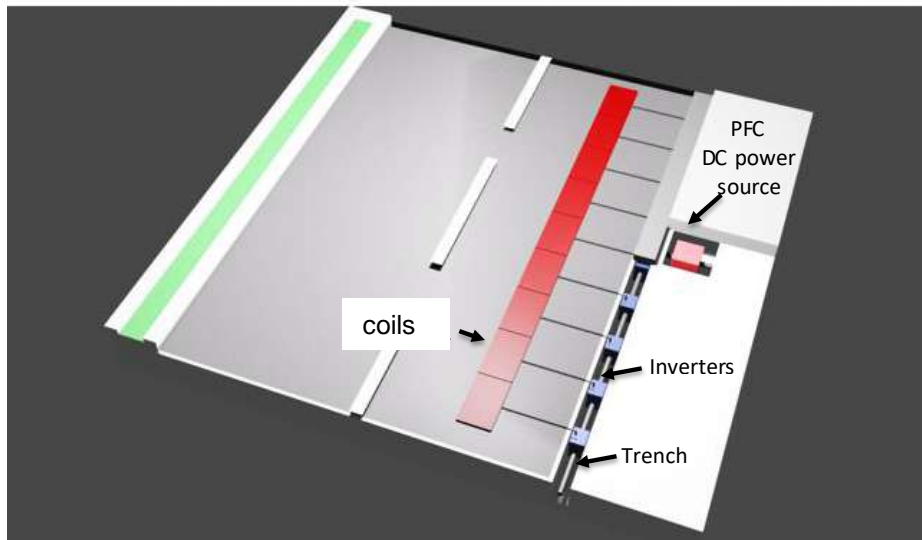


Figure 2. Layout of the charging system

Figure 3 shows a prototype of a primary coil. It consists of a frame, containing the copper wire loops, ferrite plates placed under the loops, and capacitors. The ferrite plates allow to channelize the magnetic field towards the vehicle. The frame has a void in its center to facilitate anchoring in the pavement materials. The frame is filled with a dielectric resin (not shown in the figure), which protects the coils and capacitors.

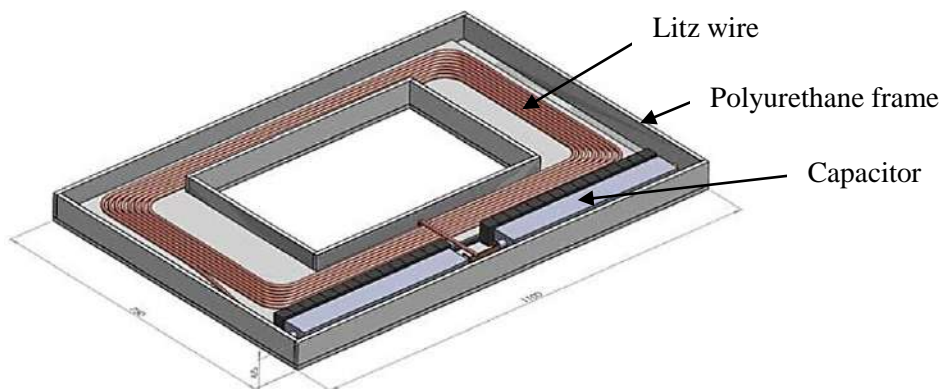


Figure 3. View of the primary coil prototype (dimensions 110 x 70 x 6.5 cm).

### 3. INTEGRATION OF THE CHARGING SYSTEM IN THE PAVEMENT

The development of a solution for the integration of the charging system in the roadway requires :

- To select suitable materials for the coil frame. These materials must have good mechanical strength, good temperature resistance, and ensure a durable seal for the coil. In particular, they must be able to protect the coil during the pavement construction phase, inducing severe loading conditions (application of hot mix and compaction).
- To define a method of installation of the coils in the pavement structure, compatible with the constraints of road construction.
- To design the system to resist to traffic loads and climatic stresses.

### 3.1. Pavement structure

The pavement structure proposed for the demonstrator is a thick bituminous pavement, composed of two high modulus asphalt base layers (11 and 10 cm thick respectively) and a 6 cm thick asphalt concrete wearing course. This structure is built on a cement-treated subgrade. The proposed solution for the installation of the coils in the pavement is described in Figure 4. It consists of :

- Milling the surface course along the entire roadway.
- Milling a trench in the middle of the base course for the installation of the coils
- Placing the coils in this trench and sealing them with a resin to ensure a good bond with the bituminous materials.
- creating a lateral micro-trench (about 5 cm wide) for the passage of the power supply cable between the coil and the inverter placed on the road side, and sealing the cable with the same resin.
- Laying a new surface course over the entire roadway.

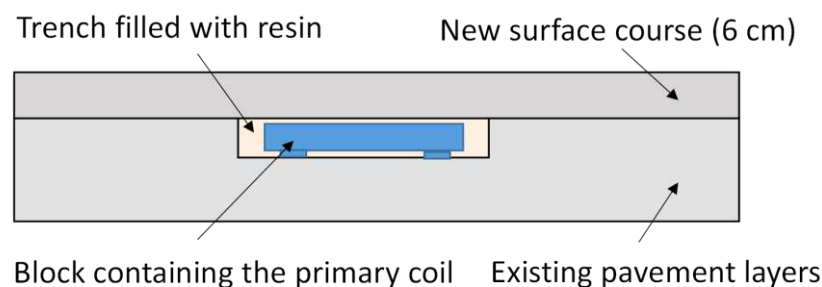


Figure 4. Solution proposed for the integration of the coils in the asphalt pavement

### 3.2. Materials

Regarding the materials, several solutions were proposed :

- For the coil block, three materials were selected: a high density polyethylene (HDPE) and two types of polyurethane, a rigid polyurethane(PUR), and a more deformable one (PUSR). These materials were recommended by the coil manufacturer, for having appropriate mechanical and dielectric properties.
- For the sealing resin, three materials were also selected: two resins used for sealing tramway rails in pavements, VA60, which is very flexible, and M95, which is slightly stiffer, and a more rigid resin, Plastiroc, used for sealing pavement cracks.
- For the new wearing course, a very thin asphalt concrete (BBTM) was chosen.

### 3.3. Methodology proposed for the validation of the pavement integration solution

To select the most appropriate materials and to evaluate the mechanical and thermal behavior of the Electric Road structure, an original approach, combining laboratory tests and modeling, was proposed. After performing classical modulus measurements on the resins (not detailed here), two types of original laboratory tests were carried out to evaluate the integration of the inductive coils in the asphalt mixes: will tracking tests, simulating the passage of wheel loads on slabs integrating small scale coil elements, and four point bending tests, on beams composed of two materials, aiming at evaluating the bonding between the resin and the coil block.



## 4. MECHANICAL PERFORMANCE TESTS

### 4.1. Wheel tracking tests

The wheel tracking test (EN 12697-22) is a standard test for evaluating the resistance to rutting of asphalt mixes. It consists of subjecting an asphalt slab of dimensions 500 x 180 x 100 mm to repeated loading, using a wheel, circulating on the surface of the slab, and applying a contact pressure of 600 kPa. This test is normally performed at a temperature of 60°C and a loading frequency of 1 Hz.

This test has been adapted in order to test plates in which a block of HDPE or PUR has been sealed, simulating the coil, in order to evaluate the resistance to traffic of this element. Figure 5 shows the test specimen. It consists of a 7 cm thick layer of asphalt concrete (BBSG), in which a 4 cm deep groove has been made. A block of plastic material simulating the coil, of dimensions 210 x 150 x 20 mm, is sealed in this groove with one of the selected resins. Finally, a 3 cm thick layer of 0/4 mm BBTM is laid on the surface. A reduced scale model of a coil integrated in the asphalt is thus obtained.

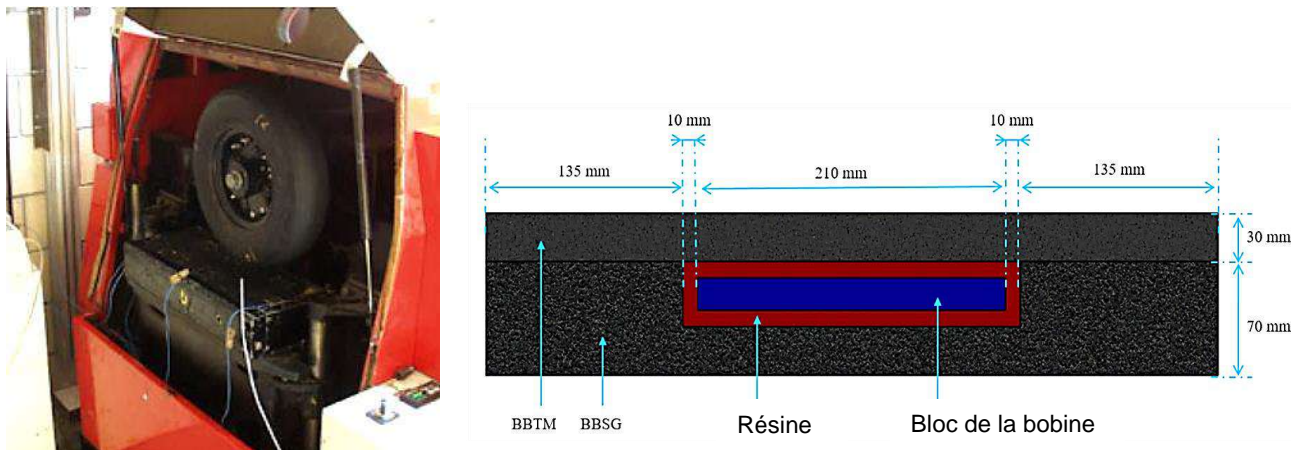


Figure 5. Principle of the wheel tracking test and geometry of the tested specimen.

Four wheel tracking tests were performed on several combinations of materials. Two specimens are tested simultaneously in each test. The test procedure consisted of applying 1000 load cycles at room temperature, and then 30,000 cycles at 60°C, and determining the evolution of the rut depth with the number of cycles. Table 1 summarizes the different tests and the maximum rut depths obtained after 30,000 cycles. According to French specifications, the maximum rut depth must be less than 10%.

Test n°1 consisted of testing two identical specimens, with an HDPE block, sealed with VA60 resin. This test led to very large rut depths, exceeding 10%. A second test (n°2) was therefore carried out to compare the rutting obtained with a specimen with an embedded coil (as in test 1), and a test specimen consisting of the two asphalt layers, without coil. These tests confirmed that the excessive rutting is, indeed, due to the integration of the coil, and not to the asphalt mixes, which present satisfactory performances (rutting of 6.5% at 30,000 cycles).

Since the coil block is made of a rigid material, it was assumed that the high rutting was mainly due to the resin used (VA60). Two other tests (n°3 and n°4) were therefore performed with the 2 other resins (M95 and Plastiroc), and also changing the material of the support

block (PUR in test 3 and PUSR in test 4). Both tests led to acceptable performances, with a slight advantage for Plastiroc, leading to slightly lower rut depths.

Table 1. Results of the wheel tracking tests.

Test	Sample	Asphalt materials	Coil block	resin	Final rut depth (%)
1	1.1	BBSG + BBTM	PEHD	VA60	15,15 %
	1.2	BBSG + BBTM	PEHD	VA60	11,5 %
2	2.1	BBSG + BBTM	sans	sans	6,50 %
	2.2	BBSG + BBTM	PEHD	VA60	12,89 % at 3000 cycles
3	3.1	BBSG + BBTM	PUR	M95	5,95 %
	3.2	BBSG + BBTM	PUR	Plastiroc	3,97 %
4	4.1	BBSG + BBTM	PUSR	M95	7,27 %
	4.2	BBSG + BBTM	PUSR	Plastiroc	4,97 %

From these results, it was concluded that the use of a very soft resin (such as VA60) could result in high vertical deformations in the asphalt wearing course, leading to high rutting. The rutting resistance could be greatly improved by using stiffer resins (M95 and Plastiroc), with the best results being obtained with Plastiroc. It was also concluded that the coil block material, which is stiffer than the resin, had little influence on rutting resistance.

#### 4.2. Evaluation of interface bonding

A good bond between all the components of the system is essential for the good performance of the pavement structure. In order to test the strength of the bond between the resins and the inductive coils, a 4-point bending test on specimens made of these two materials was developed.

Figure 6 shows the test setup. The test specimen consists of 2 beams of 80 x 50 x 20, made of the coil block material, sealed together with a 20 mm thick layer of resin. Monotonic bending tests were performed at a loading rate of 1mm/min until failure, at the laboratory ambient temperature (22+/- 1°C). The vertical force and vertical displacement were measured during loading. These tests were performed with two different interface conditions, for the coil material: a smooth interface, and a rough interface, created by sawing grooves on the contact surface. Eight 4-point bending tests were performed, varying the materials and interface conditions. Table 2 summarizes the test procedures and the results (maximum tensile stresses at failure  $\sigma_{tmax}$ ). Figure 7 shows the stress-displacement curves obtained in the different tests.

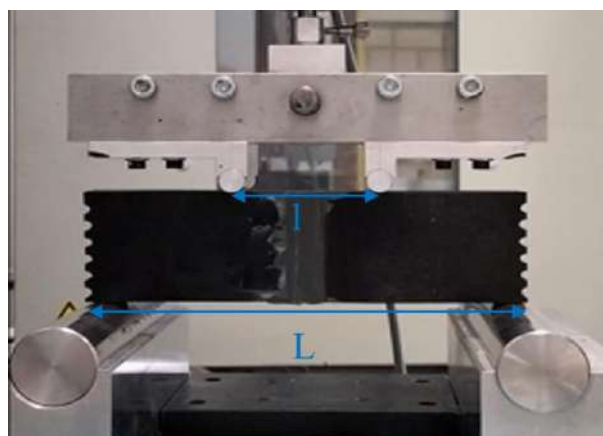


Figure 6. Test setup for the 4-point bending tests

Table 2. Results of the 4-point bending tests.

Test	$\sigma_{Tmax}$ (MPa)	Failure mode
PUSR+M95 – smooth interface	2.34	Failure in PUSR
PUSR+M95 – rough interface	2.29	No failure
PUR+M95 – smooth interface	5.87	Failure at block / resin interface
PUR+M95 – rough interface	10.21	Failure in resin
PUSR+Plastiroc – smooth interface	1.91	Failure at block / resin interface
PUSR+Plastiroc– rough interface	2.61	Failure in resin
PUR+Plastiroc – smooth interface	5.70	Failure at block / resin interface
PUR+Plastiroc– rough interface	5.99	Failure in resin

As shown in table 2, all the tests lead to high tensile stresses at failure, exceeding the tensile strength of bituminous materials (which is of the order of 1 MPa at 20°C). However, the failure strains are lower, and the failure stresses are higher with PUR, which is stiffer. Conversely, there is no clear difference between the results obtained with the 2 resins (M95 and Plastiroc). These results indicate that adhesion between the resin and the coil should not be a problem, and that the two resins tested show satisfactory adhesion. But the PUR material shows, as expected, a better mechanical resistance than the PUSR.

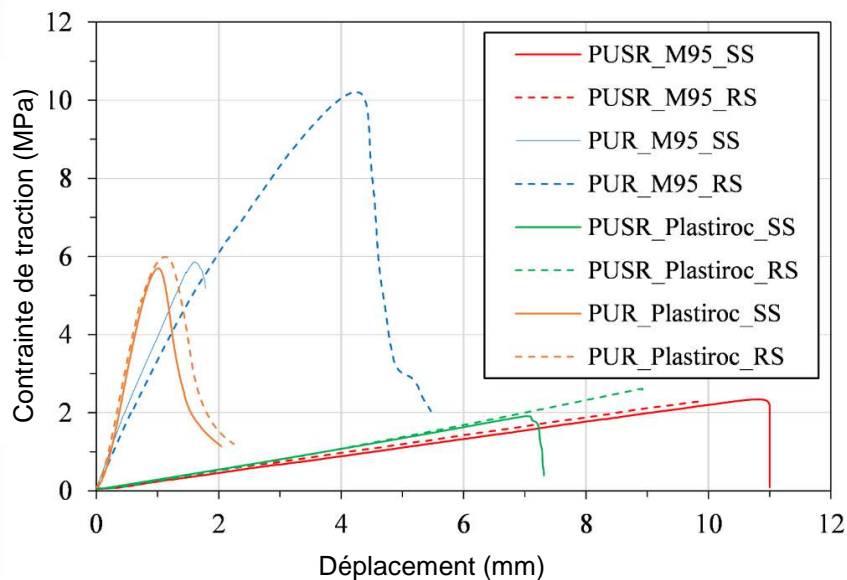


Figure 7. Tensile stress-displacement curves of the four point bending tests

## 5. MODELLING OF MECHANICAL BEHAVIOUR UNDER TRAFFIC LOADING

### 5.1. Modelling assumptions

Since laboratory tests cannot accurately reproduce the loading conditions in the pavement, modelling was carried out to simulate the mechanical behaviour of the Electric Road structure under road traffic.

A simplified model, similar to the approach used in the French pavement design method [7] was adopted. The calculations were carried out using the finite element method, with the Solidworks software, in 3D and in linear elasticity. The pavement structure considered, corresponding to the demonstrator, and the loading hypotheses, are shown in Figure 8. The pavement structure consists of a 25 cm thick asphalt base (GB3), in which the coil is

integrated; it is sealed with a one centimeter thick layer of resin. A 5 cm thick asphalt concrete wearing course (BBM) is placed on the surface. The characteristics of the materials are summarized in Table 3. For the asphalt materials, elastic moduli at 15 °C and 10 Hz were used in the calculations. Two different resins were also considered: the VA60 resin, which is very flexible, and the Plastiroc resin, which is the most rigid.

Table 3. Material characteristics used for the mechanical modelling

Material	Modulus $E$ (MPa)	Poisson ratio, $\nu$	Density $\rho$ (kg/m <sup>3</sup> )
Resin	4.34 * / 5662*	0.45	1830
Coil block (PUR)	2300	0.40	950
BBM	5400	0.35	2350
GB3	9300	0.35	2350
Subgrade PF2	50	0.35	2000

\* Elastic modulus values of the VA60 and Plastiroc resins respectively.

The load corresponds to the standard equivalent axle of the French pavement design method (single axle with dual wheels, loaded at 130 kN). The contact surfaces of the wheels are considered rectangular (see figure 8). Three loading cases have been considered, corresponding to 3 different positions of the wheels relative to the coils (figure 9):

- Coil located in the middle of the axle - this is the most frequent position, since the coils are placed in the middle of the road lane.
- Left wheels of the axle passing at the edge of the coil.
- Left wheels of the axle passing over the coil.

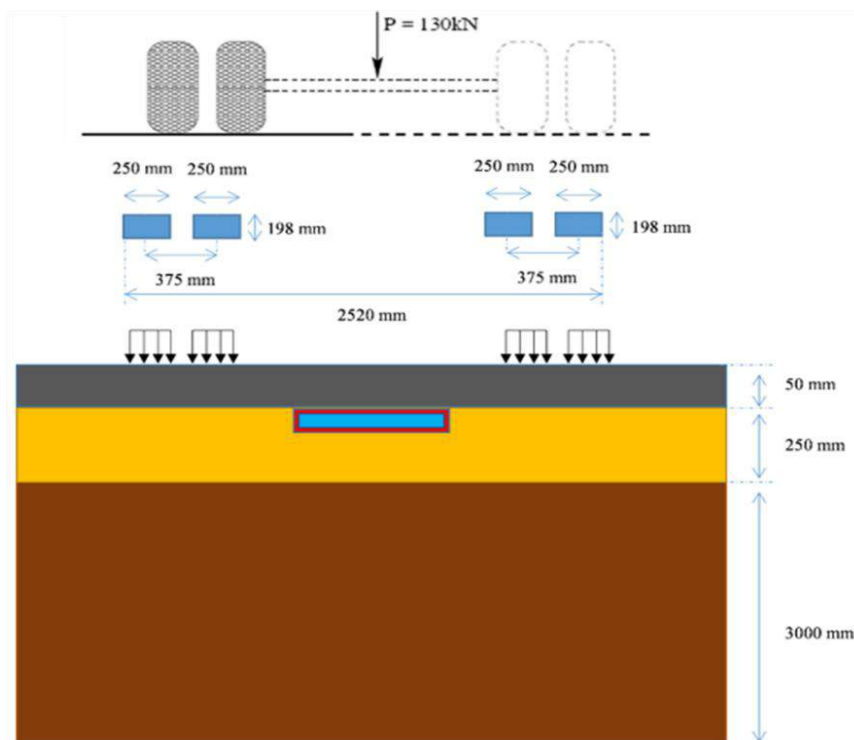


Figure 8. Pavement structure considered for the mechanical modelling



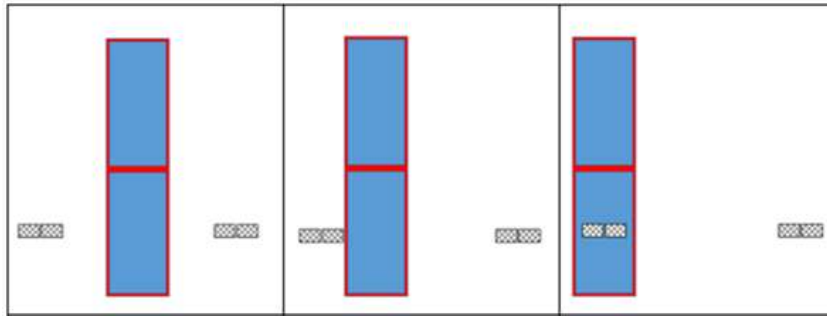


Figure 9. Different positions of the wheels relative to the coils (top view).

## 5.2. Results

Six calculations were performed for the pavement structure shown in figure 8, considering the 3 load positions, and the 2 resins, Plastiroc (loading cases 1 to 3) and VA60 (loading cases 4 to 6). The results of the first finite element calculation (with wheels located on both sides of the coil,) are presented on figure 10. This figure shows the stress and strain fields obtained in the structure: vertical stress  $\sigma_z$ , principal stress  $\sigma_1$ , and principal strain  $\epsilon_1$ . It can be seen that for this first case, the highest stresses  $\sigma_1$  are obtained at the surface, just under the wheels (negative stresses, in compression) and at the base of the GB3 layer (positive stresses, in tension). The maximum strains  $\epsilon_1$  are obtained at the base of the GB3 layer, under the wheels. For this first case, the wheel loads, located far from the coil, induce practically no stresses on the coil, and the response is almost identical to that of a conventional pavement, without any embedded charging system.

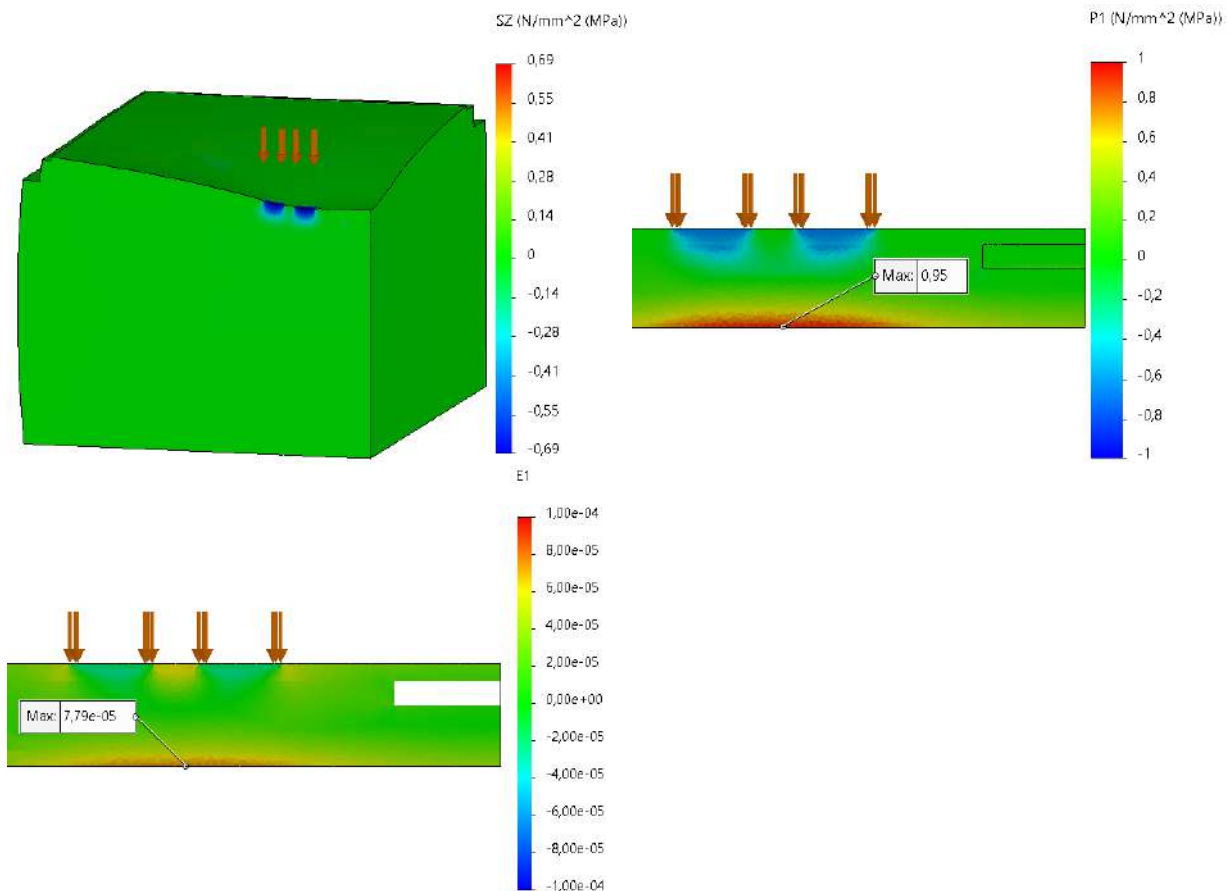


Figure 10 : Stress and strain fields calculated in the pavement structure for loading case n°1 (Plastiroc resin, coil located in the middle of the axle).

Figure 11 shows an example of strain field ( $\varepsilon_1$ ) calculated for case n°6, where the wheels are located above the coil. At this position, the results are very different : when the loads are applied directly on the coil, high strains are generated at the interface between the coil and the asphalt.

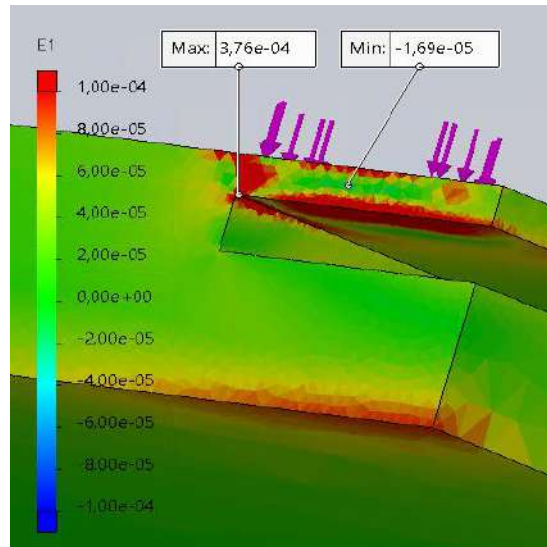


Figure 11. Variations of principal strain  $\varepsilon_1$  close to the wheel load. Loading case n°6 (VA60 resin – wheels located above the coil).

In order to assess whether the calculated stresses and strains can lead to pavement damage, an attempt was made to define failure criteria, similar to those used in the French pavement design method. Three criteria were defined for pavement materials (for a temperature of 15°C and a frequency of 10 Hz) :

- A criterion on the maximum tensile stress in the asphalt  $\sigma_{t\ ad}$ . For this criterion, a maximum value  $\sigma_{t\ ad} = 1\ \text{MPa}$  was considered.
- A criterion on the maximum tensile strain in the asphalt  $\varepsilon_{t\ ad}$ . For this criterion, the fatigue law of the French pavement design method was used; this law defines a maximum permissible strain, by the equation :

$$\varepsilon_{t,ad} = \varepsilon_6(10^\circ\text{C}, 25\ \text{Hz}) [E(10^\circ\text{C})/E(15^\circ\text{C})]^{0,5} (NE/10^6)^b \quad (1)$$

With :  $\varepsilon_6(10^\circ\text{C}, 25\ \text{Hz})$  and  $b$  parameters determined by the 2 point bending fatigue test, performed at 10 °C and 25 Hz.

$E(10^\circ\text{C})/E(15^\circ\text{C})$  the ratio of the elastic moduli at 10 °C and 15 °C.

NE the number of load cycles.

For a GB3 asphalt material, and for  $NE = 1$  million load cycles, which represents a traffic of about 100 equivalent standard axles per day during 27 years, (heavy traffic for urban streets), this leads to  $\varepsilon_{t\ ad} = 102\ \mu\text{strains}$ .

- A criterion on the maximum vertical strain  $\varepsilon_{z\ ad}$ , leading to failure of the subgrade. Based again on the French pavement design method, the maximum permissible strain was defined by equation (2):

$$\varepsilon_{z,ad} = 12000(NE)^{-0,222} \quad (2)$$

Considering again  $NE = 1$  million load cycles, this leads to :  $\varepsilon_{z\ ad} = 558\ \mu\text{strains}$ .

However, at this stage, it was not possible to define failure criteria for the resin used to seal the coil in the asphalt, and for the interfaces. Determination of the fatigue resistance of the

resin and of the interfaces would require to develop specific fatigue tests, in addition to those already developed in this study. This was not possible in this project, but could be the subject of further research.

Table 4 summarizes the maximum values of stresses and strains obtained for the three criteria defined previously ( $\sigma_1$ ,  $\varepsilon_1$ , et  $\varepsilon_z$ ), for each loading case. In this table, the values indicated in red exceed the permissible values.

Table 4. Maximum stress and strain values in the pavement structure, pour for the six loading cases.

Loading case	1	2	3	4	5	6
<b>Resin</b>	Plastiroc			VA60		
$\sigma_1$ : Maximum principal stress in GB3 (MPa)	0.95	0.95	1.0	0.954	1.03	2.85
$\varepsilon_z$ : maximum vertical strain in subgrade ( $\mu\text{def}$ )	-274	-280	-301	-287	-313	-349
$\varepsilon_1$ : maximum principal strain in GB3 ( $\mu\text{strain}$ )	77	77	80	80	130	865

Table 4 shows that in the calculations performed with the Plastiroc resin, the stresses and strains never exceed the permissible values, and vary little with the position of the wheels. This is due to the small difference in moduli between the Plastiroc (5662 MPa), the BBM (5400 MPa) and the PUR coil block (2300 MPa), which does not lead to any stress or strain concentration. On the contrary, with the highly flexible VA60 resin, a significant increase in maximum tensile stresses ( $\sigma_1$ ) and maximum tensile strains ( $\varepsilon_1$ ) is observed in the asphalt layers, when the wheels are located at the edge of the coil (case n°5) and even more when they are located above the coil (case n°6). These results indicate risks of cracking or failure when the wheels pass close to the coil or over it. However, this will only occur occasionally, when the vehicle moves laterally or changes lanes. The stresses and strains remain all acceptable when the vehicle is centered in the lane (case n°4).

These results agree with the conclusions of the laboratory rutting tests [§ 4.1], which indicated that a large difference in stiffness between the asphalt materials and the inclusions can generate high stress and strain levels, and subsequent distresses. This also confirms that the flexible resin, VA60, is not suitable for sealing the inductive coils.

## 6. MODELLING OF THERMAL BEHAVIOUR

### 6.1. Modelling assumptions

One important characteristic of inductive charging systems is that, due to their high charging power (here 30 kW), they produce significant heat dissipation, by Joule effect. This heat dissipation can lead to an increase in temperature, which could cause rutting of bituminous materials, when the ambient temperature is high (in summer). In order to evaluate this temperature increase, finite element simulations of the thermal behaviour were carried out. The calculations were performed in 2D, with the Cast3M® software, taking into account the temperature variations in the pavement due to climatic conditions, and the heat loss in the inductive coils.

The simulations were carried out for a pavement structure similar to that used for the mechanical modelling, shown in Figure 12. This structure comprises a 25 cm thick GB3 asphalt base, in which the coil is integrated, and a 5 cm thick BBM wearing course. This

structure rests on a 3 m thick granular subgrade. For the thermal modelling, only the thermal properties of the materials, thermal conductivity, heat capacity and density are taken into account; they are summarized in Table 5. In the calculations, null heat flux boundary conditions are considered at the base of the model, and on the lateral sides. The upper side of the model is subjected to climatic variations, and 3 types of heat exchanges are considered:

- Solar radiation (direct and diffuse).
- Convection with air.
- Longwave radiation (radiation heat transfer between the structure and the sky).

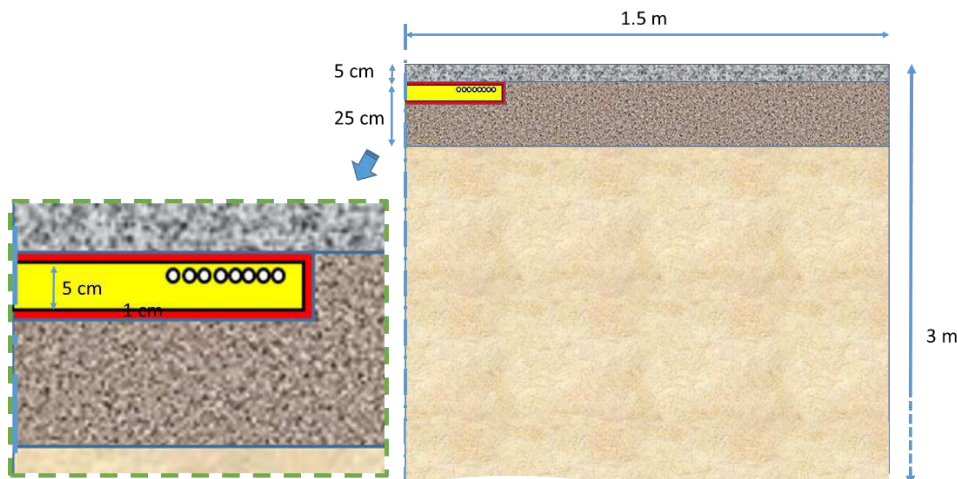


Figure 12. Pavement structure considered for the thermal simulations

Table 5. Thermal characteristics of the materials

	Thermal conductivity [W/m/°C]	Heat capacity [J/°C/kg]	Density [Kg/m <sup>3</sup> ]
BBM	2.	869	2480
BBSG	1.9	869	2350
Subgrade	2.	869	1800
PUR	0.42	1330	1530
Plastiroc resin	0.82	966	1830

The thermal calculations were performed for conditions representative of a summer day in Paris, with a maximum ambient temperature of 28°C, a low wind speed of 2 m/s, and a clear sky. The solar radiation was calculated for conditions corresponding to the summer solstice, with a half-sinus daily variation. The maximum solar radiation, corresponding to the latitude of Paris, was taken equal to 1075 W/m<sup>2</sup>. Considering an albedo of the surface layer of 0.15, this leads to a maximum radiation received by the pavement of 914 W/m<sup>2</sup>. The heat flux received by the structure (over 2 consecutive days) is shown in Figure 13. For the ambient temperature, a sinusoidal variation was considered, with a maximum temperature of 28°C during the day and a minimum temperature of 18°C at night (see also figure 13).

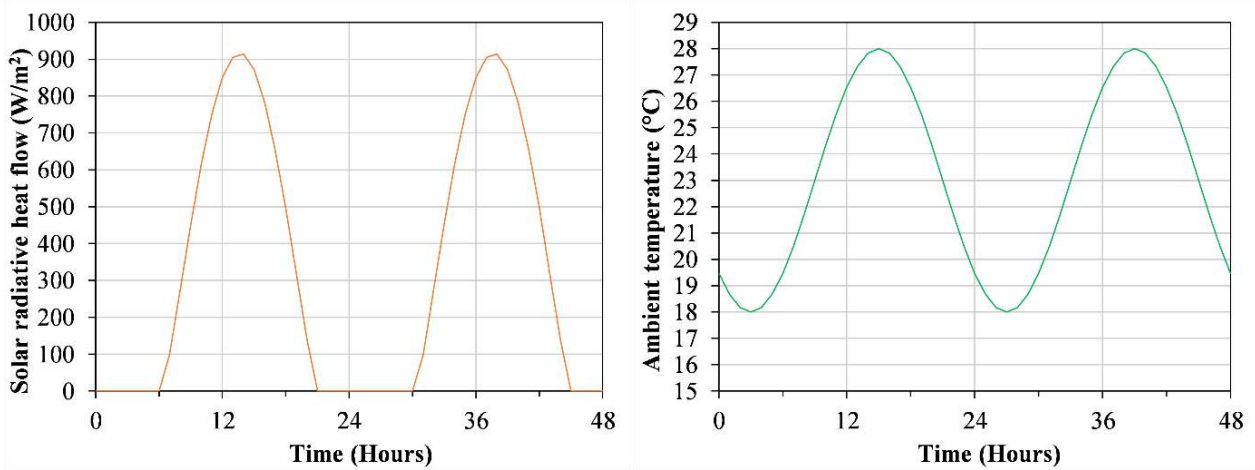


Figure 1 : Heat flux ( $W/m^2$ ) and air temperature variations considered in the thermal calculations.

The heat flux  $Q_{conv}$  exchanged by convection is calculated by equation 1, where  $h_{conv}$  is the convective transfer coefficient, calculated with the model proposed by Nusselt and Jürges [8] (equation 2).

$$Q_{conv} = h_{conv} \times (T_{surface} - T_{ambient}) \quad (1)$$

$$h_{conv} = 4,0 \times v_{wind} + 5,6 \quad \text{for } v_{wind} \leq 5 \text{ m/s} \quad (2)$$

With  $v_{wind}$  the wind speed in m/s. For a wind speed of 2 m/s, this leads to a convective transfer coefficient  $h_{conv} = 13.6 \text{ W/m}^2/\text{K}$ .

Finally, the re-emitted long wave radiation  $Q_{LWR}$  is calculated by equation 3 :

$$Q_{LWR} = \varepsilon \times \sigma \times (T_{surface}^4 - T_{sky}^4) \quad (1)$$

With:  $\sigma$ : the Stefan-Boltzmann constant:  $5.67 \times 10^{-8} \text{ W/m}^2/\text{K}^4$ .

$\varepsilon$ : the emissivity of the pavement surface.

$T_{surface}$ : the surface temperature (K)

$T_{sky}$ : the sky temperature (K)

## 6.2. Heat flux emitted by the inductive coils

In the thermal model, the Litz wire loops of the coil are represented by circular holes (in 2D). The heat flux, due to Joule effect losses, is applied to the borders of these holes. With a coil power of 30 kW, this heat flux has been estimated at 300 W by VEDECOM.

The thermal calculations were performed for 2 consecutive days. On the first day, only the climatic variations were taken into account; the heat flux due to the inductive coils was only activated on the second day, between 6 am and 6 pm. Furthermore, since the operation of the coils is intermittent, different coil operating times were considered corresponding to 20%, 30% and 50% of the total time, representing very intensive charging conditions.

## 6.3. Results

Three thermal simulations were performed, with the assumptions presented in sections 6.1 and 6.2, simulating high temperature summer conditions. Each calculation covers a period of 2 days (48 hours), with the coil functioning only on the second day, between 6 am and 6 pm. Figure 14 shows the maximum temperature variations obtained in the coil block and in the asphalt layers. The results show that the heat flux generated by the coil increases considerably the temperatures in the PUR and in the asphalt, during the second day,



compared to the effect of the climatic conditions alone. Depending on the percentage of time the coil is running, the following maximum temperatures are attained:

- 68°C in the PUR and 63°C in the asphalt for a charging rate of 20 %.
- 80 °C in the PUR and 70 °C in the asphalt for a charging rate of 30 %.
- 103°C in the PUR and 83°C in the asphalt for a charging rate of 50 .

To complete the previous results, Figure 15 shows the maximum temperature distribution obtained around the coil, for an operating time of 30%. The highest temperatures (above 60°C), are located in a limited area, around the coil cables.

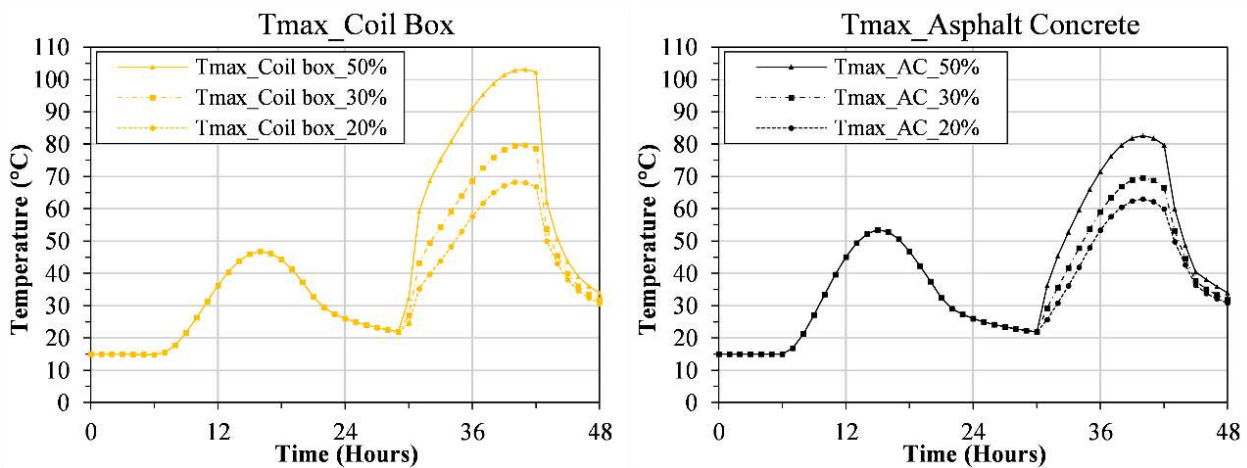


Figure 2. Maximum temperature variations obtained in the coil block and in the asphalt, for different percentages of coil charging time.

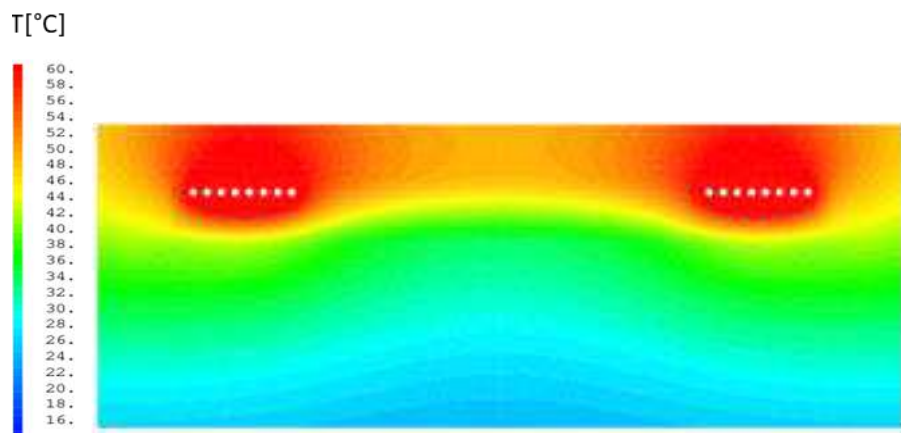


Figure 14. Maximum temperature field around the coil for 30% of charging time.

In conclusion, the results of the thermal modelling show that under intensive operating conditions, the coil block and the asphalt could reach high temperatures during hot summer periods. For the coil, this implies the need to use materials able to resist to temperatures of about 100°C. For the pavement, this means using asphalt materials with high resistance to rutting, or even changing for other types of materials, such as concrete, in hot climates. It also confirms the need to install temperature sensors on the future demonstrator, to monitor actual operating temperatures, to validate the modelling results. A complementary measure could consist of installing a shut-down system, to stop charging in case of excessive temperatures.

## 7. CONCLUSIONS

This article presents first studies carried out in the European INCIT-EV project, to develop solutions for the integration of inductive charging systems in an asphalt pavement. Designing such an Electric Road raises new issues, related to the integration in the pavement of materials with different mechanical and thermal properties, and to the heating caused by the coils, which can significantly increase the temperatures in the pavement. To address these issues, specific test methods and numerical models have been proposed.

Laboratory wheel tracking tests, on small-scale models, have shown the great influence of the stiffness of the elements integrated into the pavement, and in particular of the resin used for sealing the coil, on rutting behaviour. They have shown that a very flexible resin contributes to increasing the rutting of the asphalt layers. Four-point bending tests were also carried out to evaluate the bond between the resin and the block containing the coil. These tests allowed to compare different solutions and to select a suitable resin (Plastiroc) for sealing the coils in the pavement.

In addition, mechanical and thermal modelling was carried out to simulate the behaviour of the coils in a bituminous pavement structure. The mechanical modelling indicated that to limit risks of deterioration, the elements integrated in the road must have mechanical properties as close as possible to those of the pavement materials. This result is consistent with the rutting tests. These calculations also showed that high stresses are generated only when the loads are applied directly on the coils, or at their edge. Such situations will occur only occasionally, if the vehicles move laterally, or change lanes.

Thermal simulations have shown that the high charging power of the inductive coils (30 kW) can lead to significant heating. Under adverse conditions (intensive operation of the coils, and hot weather), this could lead to high temperatures, exceeding 60 °C, in the pavement, and to risks of rutting. Depending on the conditions of use, appropriate materials need to be chosen, to avoid such damage.

The results presented in this article represent a first study, at laboratory scale, for the development of the Electric Road demonstrator to be built in Paris. Before the construction of the demonstrator, full-scale accelerated loading tests will be performed, with the FABAC linear traffic simulator of Université Gustave Eiffel, to validate the results obtained in the laboratory tests and in the numerical simulations.

## ACKNOWLEDGEMENTS

This research has been carried out as part of the INCIT-EV project, which has received funding from the European Union's Horizon 2020 research and innovation programme under grant agreement No. 875683

## REFERENCES

1. INCIT-EV, A european project on innovative charging technologies based on the user's perception of electric mobility," 2020-2023, <https://www.incit-ev.eu>
2. F. Chen, N. Taylor, and N. Kringos, "Electrification of roads: Opportunities and challenges," *Applied Energy*, vol. 150, pp. 109–119, 2015.
3. D. Bateman, D. Leal, S. Reeves, M. Emre, L. Stark, F. Ognissanto, R. Myers, and M. Lamb, "Electric road systems: A solution for the future?," tech. rep., 2018
4. Simonin J.M., Hornych P., Nguyen M.L. (2017), Bibliographie sur les technologies pour l'implantation de systèmes de recharge des véhicules électriques dans les chaussées, rapport du projet ADEME E-Way Corridor, 37p, Avril 2017.
- 5.

6. F. Chen, Sustainable implementation of electrified roads: structural and material analyses. PhD thesis, KTH Royal Institute of Technology, 2016
7. Hornych P., Gabet T., Mazhoud B., Meira Z., Kadem K., Delfosse E., Coquelle E. (2022), Road Infrastructure upgrading for dynamic wireless charging, rapport D 4.10 du projet INCIT-EV, 104 p.
8. J.-F. Corté and M.-T. Goux, "Design of pavement structures: the French technical guide," Transportation Research Record, vol. 1539, no. 1, pp. 116–124, 1996.
- 8 W. Jürges, "The heat transfer at a flat wall (der wärmeübergang an einer ebenen wand), beihefte zum gesundh," Ing, vol. 1, p. 19, 1924.